Submitted to

14th International Workshop on Deep Inelastic Scattering, DIS2006, April 20-24, 2006, Tsukuba, Japan

www-h1.desy.de/h1/www/publications/conf/conf_list.html

H1prelim-06-011

A New Measurement of Exclusive ρ^0 Meson Photoproduction at HERA

H1 Collaboration

Abstract

Using a sample of more than 240000 events taken with the H1 detector at HERA in 2005, a new measurement of exclusive ρ^0 photoproduction in the kinematic range $20 < W < 90\,\mathrm{GeV}$ and $|t| < 3\,\mathrm{GeV}^2$ is performed. From the measurement of the W dependence of this process in eight bins of t, the Pomeron trajectory $\alpha_{\mathbb{P}}(t)$ can be extracted for the first time from the data of a single experiment. The result is $\alpha_{\mathbb{P}}(t) = 1.093 \pm 0.003(stat.)^{+0.008}_{-0.007}(syst.) + (0.116 \pm 0.027(stat.)^{+0.036}_{-0.046}(syst.))\,\mathrm{GeV}^{-2} \cdot t$.

1 Introduction

The exclusive photoproduction of ρ^0 mesons has been studied in great detail over the last 40 years [1, 2, 3, 4, 5, 6, 7]. This process shows the typical characteristics of a diffractive reaction, i.e. a weak growth of the cross section with the photon-proton centre-of-mass energy W and an exponential decrease as function of the modulus of the squared momentum transfer $|t|$.

This behaviour can be understood in terms of the vectormeson dominance model (VDM) [8], where the hadronic part of the photon wavefunction is conceived as a superposition of vector–meson states, in which the contribution from the ρ^0 dominates. This hadronic component of the photon may then participate in hadron–hadron interactions, notably in elastic scattering off the proton.

Thus, an understanding of ρ^0 photoproduction sheds light on the hadronic properties of the photon, including the total photon–proton cross section, which is linked to the elastic scattering amplitude by the optical theorem.

At sufficiently high centre-of-mass energies W, elastic hadron-hadron scattering is well described by the exchange of a single Regge trajectory [9], the Pomeron, while at lower values of W the exchange of additional meson trajectories becomes important. The contribution of the exchange of these so-called subleading trajectories to the production cross section is often summed up by introducing an effective Regge trajectory, the Reggeon.

In this high–W region, where Pomeron exchange is dominant, the energy dependence of elastic ρ^0 photoproduction at fixed momentum transfer t is in diffractive models directly linked to the Pomeron trajectory $\alpha_{\mathbb{P}}(t)$ by

$$\frac{\mathrm{d}\sigma_{\gamma\mathrm{p}}(W)}{\mathrm{d}t} \propto \left(\frac{W}{W_0}\right)^{4(\alpha_{\mathbb{P}}(t)-1)} .$$

Thus, a measurement of the W dependence of elastic ρ^0 photoproduction in bins of t is paramount to the direct measurement of the Pomeron trajectory $\alpha_{\mathbb{P}}(t)$, which is well approximated by a linear function $\alpha_{\mathbb{P}}(t) = \alpha_{\mathbb{P},0} + \alpha'_{\mathbb{P}} \cdot t$.

The ZEUS collaboration has measured ρ^0 photoproduction cross sections [7] at high values of $W \approx 94\,\mathrm{GeV}$, and has combined its data with data taken at lower energies [2] and with earlier HERA data from H1 [4] and ZEUS [3, 6] in order to extract the W dependence of ρ^0 photoproduction and thus the Pomeron trajectory. Their result is $\alpha_{\mathbb{P}}(t) = (1.096 \pm 0.021) + (0.125 \pm 0.038)\,\mathrm{GeV}^{-2} \cdot t$. The intercept $\alpha_{\mathbb{P},0}$ is consistent with the expectations of Donnachie and Landshoff [10] ($\alpha_{\mathbb{P},0} = 1.0808$) and Cudell [11] ($\alpha_{\mathbb{P},0} = 1.096^{+0.012}_{-0.009}$), whereas the measured slope $\alpha'_{\mathbb{P}}$ is significantly lower than the canonical value of $\alpha'_{\mathbb{P}} = 0.25\,\mathrm{GeV}^{-2}$ extracted from other diffractive processes [12].

In the present analysis, we measure the W dependence of diffractive ρ^0 photoproduction over an extended W range of $20 < W < 90\,\mathrm{GeV}$ in bins of t within a single experiment. Thus we can extract the Pomeron trajectory from the data of one experiment alone, which reduces the uncertainty from different systematic errors of different experiments. The ρ^0 meson is identified by its decay to two charged pions, which has a branching ratio of $99\,\%$.

2 Event Selection and Triggering

The data were taken with the H1 detector in 2005, when HERA collided $920\,\mathrm{GeV}$ protons with $27.6\,\mathrm{GeV}$ positrons. The H1 detector has been described in detail elsewhere [13]. A detailed description of the analysis can be found in [14].

Events were mainly triggered with the Fast Track Trigger (FTT) [15] at the first H1 trigger stage (trigger level 1). This trigger combines track segments, which are identified in four three-wire-groups within the central jet chamber (CJC), to track candidates within the trigger level 1 decision time of $2.3\,\mu\mathrm{s}$. Two out of four possible track segments have to be identified and found to correspond to compatible track parameters (signed curvature and azimuth) in order to form a track at level 1. Tracks with transverse momenta as low as $100\,\mathrm{MeV}$ can be identified. Events were triggered if two or three tracks were found by the FTT with a total charge of zero or ± 1, and if at least two of the tracks had a transverse momentum above $160\,\mathrm{MeV}$.

In addition, a trigger signal from the inner proportional chamber (CIP) trigger, consistent with a low multiplicity interaction in the nominal interaction region, was demanded. Events with large energy deposits in the inner forward part of the Liquid Argon (LAr) calorimeter or signals in a set of scintillators (FTI2) within the forward tracker were rejected.

The data were taken during a period of three months in 2005, when the operation parameters of the FTT and the CJC were stable. Correcting for the trigger prescale, the data correspond to an integrated luminosity of $569.7\,\mathrm{nb}^{-1}$.

In order to identify events where the ρ^0 decays to $\pi^+\pi^-$, events were selected by demanding:

- A reconstructed primary vertex within $25\,\mathrm{cm}$ of the nominal interaction point in z,
- exactly two primary vertex fitted tracks of opposite charge in the central detector, with transverse momenta above $200\,\mathrm{MeV}$ and polar angle within the range $20^\circ < \theta < 160^\circ$, of good quality,
- no additional tracks in the central or forward tracker,
- no scattered electron candidate in the LAr or SpaCal calorimeters,
- no calorimeter custers with energies above $500\,\mathrm{MeV}$ that are not associated with one of the pion tracks. A cluster is considered to be associated with a track when the distance in pseudorapidity η and azimuthal angle ϕ is less than 0.175.

A total of $271'684$ events passed these selection criteria, $241'672$ of these events lie in the mass range $0.6 < m_{\pi\pi} < 1.1\,\mathrm{GeV}$, where $m_{\pi\pi}$ is the invariant mass of the two tracks under a charged pion mass hypothesis.

The four-vectors of the two decay pions are reconstructed from their measured track momenta, the ρ^0 four vector is the sum of the two pions momenta.

The momentum transfer t is then calculated from the ρ^0 meson's transverse momentum:

$$t = -p_{\mathrm{t},\rho}^2$$

The γp centre-of-mass energy is calculated from

$$W = \sqrt{2E_{\mathrm{p}}(E_\rho - p_{\mathrm{z},\rho})},$$

where $E_{\mathrm{p}} = 920\,\mathrm{GeV}$ is the proton beam energy.

3 Monte Carlo Modelling

The elastic and proton-dissociative ρ^0 production was modeled using the Monte Carlo generator DIFFVM [16]. The generator models vector meson production based on the equivalent photon approximation [17], the vector meson dominance model [8], and pomeron exchange [18].

The generator models the diffractive dissociation of the proton according to a model where the mass M_{Y} of the dissociative system is generated according to

$$\frac{\mathrm{d}^2\sigma}{\mathrm{d}t\,\mathrm{d}M_{\mathrm{Y}}^2} \propto \frac{f\,(M_{\mathrm{Y}})}{(M_{\mathrm{Y}}^2)^{1+\epsilon}},$$

with $\epsilon = 0.0808$, where $f\,(M_{\mathrm{Y}})$ is a function fitted to experimental data [18] that parametrizes deviations in the low mass region $M_{\mathrm{Y}} < 1.9\,\mathrm{GeV}$ from a pure $1/(M_{\mathrm{Y}}^2)^{1+\epsilon}$ behaviour. For this low mass region, the dissociating system is treated as a N^* resonance that decays according to the measured branching fractions [19]. In the higher mass region, the system is modeled as a quark–diquark system, where the quark is assumed to be scattered out of the proton, and the fragmentation is performed using the Lund fragmentation as implemented in JETSET [20].

The Monte Carlo events were reweighted in the variables t, W, and $m_{\pi\pi}$ in order to get the best possible description of the experimentally observed distributions.

In particular, the dipion mass spectrum was reweighted from a nonrelativistic Breit–Wigner function (as implemented in DIFFVM) to a skewed relativistic Breit–Wigner function according to the model by Ross and Stodolsky [21], with the skewing parameter given by

$$n\,(t) = 6.1 \cdot \exp\,(t \cdot 1.95\,\mathrm{GeV}^{-2});$$

this parametrisation was derived from a fit to ZEUS data [6].

The t spectrum was generated as a purely exponential spectrum, and reweighted to the form

$$\frac{\mathrm{d}\sigma^{\gamma p}}{\mathrm{d}t} \propto \exp\,\left(a \ln\,(1 - b_0 t/a)\right)$$

which smoothly interpolates between an exponential decrease $\mathrm{d}\sigma^{\gamma p}/\mathrm{d}t \propto \exp(b_0 t + b_0^2 t^2/2a)$ with $b_0 = 11.4\ (6.5)\,\mathrm{GeV}^{-2}$ for $W_0 = 90\,\mathrm{GeV}$ at low values of $|t|$, and a power–law behaviour $\mathrm{d}\sigma^{\gamma p}/\mathrm{d}t \propto |t|^{-a}$ with $a = 23\ (8.5)$ at large $|t|$ for elastic (proton-dissociative) ρ^0 production. The coefficient a has been determined from fits to large-$|t|$ data for the proton-dissociative data, and from fits of the form $\mathrm{d}\sigma^{\gamma p}/\mathrm{d}t \propto \exp(b_0 t + c_0 t^2)$ [6] for elastic data.

The DIFFVM generator produces events with all values of Q^2 and M_{Y}. Events were counted as signal events if they fulfilled the cuts $Q^2 < 4\,\mathrm{GeV}^2$ and $(M_{\mathrm{Y}}^2 + Q^2)/(W^2 + Q^2) < 0.01$, otherwise they were treated as background.

4 Cross Section Determination

4.1 Corrected Number of ρ^0 Mesons

The events are distributed in 80 bins[1] in W and t: In t, there are 12 bins from $|t| = 0\,\mathrm{GeV}^2$ to $|t| = 3.5\,\mathrm{GeV}^2$. For $|t| < 0.16\,\mathrm{GeV}^2$ ($|t| > 0.16\,\mathrm{GeV}^2$), there are 10 (5) W bins for each t bin. The W range covered varies with t; as $|t|$ rises, the lower (upper) value of W changes from $20\,\mathrm{GeV}$ ($69\,\mathrm{GeV}$) to $25\,\mathrm{GeV}$ ($90\,\mathrm{GeV}$).

For each W/t bin, the number of events is evaluated in dipion mass bins of $25\,\mathrm{MeV}$ width. This dipion mass spectrum is corrected for acceptance, reconstruction and trigger efficiency, and fitted. The overall correction factor is typically 0.25. The correction factors that are applied are determined for each $m_{\pi\pi}$ bin in each W/t bin individually.

It is well known that due to the large width of the ρ meson there is a significant interference between resonant ρ production with a subsequent decay to two pions, and nonresonant dipion production. This interference leads to a distortion of the observed dipion mass spectrum. Two models have been put forward to describe this effect: The ansatz of Söding [22] describes the distorted spectrum as sum of three terms, a relativistic Breit–Wigner function for the ρ, a term for the nonresonant dipion production (here taken to be constant as function of $m_{\pi\pi}$), and an interference term:

$$\frac{\mathrm{d}N}{\mathrm{d}m_{\pi\pi}} = \frac{N_0 m_\rho \Gamma_\rho m_{\pi\pi} + I(m_\rho^2 - m_{\pi\pi}^2)}{(m_\rho^2 - m_{\pi\pi}^2)^2 + m_\rho^2 \Gamma_\rho^2} + B, \tag{1}$$

where N_0, I, and B parametrize the contributions from resonant ρ^0 production, interference, and background, respectively. Here, m_ρ is the nominal ρ^0 mass, and

$$\Gamma_\rho = \Gamma_{\rho,0} \left(\frac{m_{\pi\pi}^2 - 4m_\pi^2}{m_\rho^2 - 4m_\pi^2} \right)^{\frac{3}{2}} \frac{m_\rho}{m_{\pi\pi}}$$

is the mass dependent width of the ρ^0, following the suggestion of Jackson [23] ($\Gamma_{\rho,0}$ is the nominal ρ^0 width, and m_π the charged pion mass). In the ansatz of Ross and Stodolsky [21], a relativistic Breit–Wigner function is multiplied by a skewing term $(m_{\pi\pi}/m_\rho)^{-n}$, where m_ρ is the nominal ρ meson mass, and n is the so-called skewing parameter:

$$\frac{\mathrm{d}N}{\mathrm{d}m_{\pi\pi}} = N_0 \frac{m_\rho \Gamma_\rho m_{\pi\pi}}{(m_\rho^2 - m_{\pi\pi}^2)^2 + m_\rho^2 \Gamma_\rho^2} \left(\frac{m_\rho}{m_{\pi\pi}} \right)^n + B. \tag{2}$$

In each of the W/t bins, the corrected dipion mass spectrum $\mathrm{d}N^{\mathrm{corr}}/\mathrm{d}m_{\pi\pi}$ (in $25\,\mathrm{MeV}$ bins) is fitted in the range $0.6\,\mathrm{GeV} < m_{\pi\pi} < 1.1\,\mathrm{GeV}$ with a skewed relativistic Breit–Wigner function as proposed by Ross and Stodolsky, with the nominal ρ^0 mass and width fixed to the values $m_{\rho^0} = 766.4\,\mathrm{MeV}$ and $\Gamma_{\rho,0} = 145\,\mathrm{MeV}$, which are the average values of the corresponding fit quantities, obtained from fits in all 80 W/t bins. These values are compatible with the PDG values [19] $m_\rho = 768.5 \pm 1.1\,\mathrm{MeV}$ and $\Gamma_{\rho,0} = 150 \pm 3\,\mathrm{MeV}$. Fits where the mass and width are left as free parameters result in compatible values for m_ρ and $\Gamma_{\rho,0}$ in all W/t bins. The average values of m_ρ and $\Gamma_{\rho,0}$ derived from these fits are $m_\rho = 766.4\,\mathrm{MeV}$ and $\Gamma_{\rho,0} = 145\,\mathrm{MeV}$.

[1] Called "W/t bins" herafter.

To extract the number of resonantly produced ρ^0 mesons in each W/t bin, the integral of the unskewed Breit–Wigner function is evaluated in the region $2m_\pi < m_{\pi\pi} < m_\rho + 5\Gamma_{\rho,0}$, with the value of $m_\rho + 5\Gamma_{\rho,0} = 1.52\,\mathrm{GeV}$ taken from the PDG [19]:

$$N_{\mathrm{cor}} = N_0 \int\limits_{m_{\pi\pi}=2m_\pi}^{m_\rho+5\Gamma_{\rho,0}} \frac{m_\rho\,\Gamma_\rho\,m_{\pi\pi}}{(m_\rho^2 - m_{\pi\pi}^2)^2 + m_\rho^2\Gamma_\rho^2}\mathrm{d}m_{\pi\pi}.$$

Extracting the number of ρ^0 mesons from the corresponding term in the Söding parametrisation leads to compatible results.

There exists a different convention for the ρ^0 cross section due to Spital and Yennie [24], used e. g. by the Omega collaboration [2], who define the cross section by

$$\frac{\mathrm{d}\sigma}{\mathrm{d}t} = \frac{\pi\Gamma_{\rho,0}}{\pi} \left.\frac{\mathrm{d}^2\sigma}{\mathrm{d}t\,\mathrm{d}m_{\pi\pi}}\right|_{m_{\pi\pi}=m_\rho}.$$

For the PDG values of m_ρ and $\Gamma_{\rho,0}$, this definition leads to a cross section which is larger by a factor of 1.050 than the one derived with our definition.

To calculate the photoproduction cross section, the ep cross section is divided by the photon flux, integrated over the respective W range, and over Q^2 up to $Q^2 = 4\,\mathrm{GeV}^2$.

The average Q^2 value of the events that pass the selection, as determined from Monte Carlo studies, is $0.010\,\mathrm{GeV}^2$; it rises from $0.003\,\mathrm{GeV}^2$ for the lowest t bins to $0.4\,\mathrm{GeV}^2$ for the highest t bins. For the t bins that are used to extract the elastic cross section ($|t| < 0.7\,\mathrm{GeV}^2$), the average Q^2 value is $0.0078\,\mathrm{GeV}^2$.

4.2 Background

The following background sources were investigated:

- ϕ meson production,
- ω meson production,
- $\rho(1450)$ and $\rho(1700)$ meson production with subsequent decay to $\pi^+\pi^-\pi^0\pi^0$,
- ρ^0 meson production outside the signal range of $Q^2 < 4\,\mathrm{GeV}^2$ and $(M_{\mathrm{Y}}^2 + Q^2)/(W^2 + Q^2) < 0.01$.

The background from $\phi \to K^+K^-$ is completely negligible, as the reconstructed dipion mass is always below $0.6\,\mathrm{GeV}$, the same holds for $\phi \to K_{\mathrm{L}}^0 K_{\mathrm{S}}^0$ with subsequent decay $K_{\mathrm{S}}^0 \to \pi^+\pi^-$.

The bulk of events from $\omega \to \pi^+\pi^-\pi^0$ also has dipion masses below $0.6\,\mathrm{GeV}$, while the contribution from $\omega \to \pi^+\pi^-$ is small and manifests itself mainly through the ρ–ω interference, which has been neglected, following the procedure of earlier measurements [2, 6].

The amount of background from ρ' decays ($\rho(1450)$ and $\rho(1700)$ can be estimated from the dipion mass spectrum, which shows an indication for $\rho' \to \pi^+\pi^-$ decays in the expected mass region around $m_{\pi\pi} \approx 1.6\,\mathrm{GeV}$ at a level of $0.5\,\%$ compared to $\rho^0 \to \pi^+\pi^-$. The Crystal Barrel collaboration has measured [25] the ratio $BR(\rho' \to 4\,\pi)/BR(\rho' \to \pi^+\pi^-)$ to be 0.37 ± 0.10 for $\rho(1450)$ and 0.16 ± 0.04 for $\rho(1700)$; however, the channel $\rho' \to 4\pi$ is expected to be dominated by $2\pi^+2\pi^-$, whereas $\pi^+\pi^-2\pi^0$ is significantly smaller [26].

From these arguments, we estimate the background from ϕ, ω, and ρ' production to be smaller than $2\,\%$ and assign a corresponding normalisation uncertainty to the result.

Background from ρ^0 production outside the kinematical signal definition used in the present analysis, i.e. $Q^2 < 4\,\mathrm{GeV}^2$ and $(M_\mathrm{Y}^2 + Q^2)/(W^2 + Q^2) < 0.01$, was included in the Monte Carlo simulation and has been corrected for in the overall reconstruction efficiency.

4.3 Separation of Elastic and Proton–Dissociative Processes

To discriminate between events where the proton stays intact (elastic production) or dissociates diffractively into a state of mass M_Y, signals in additional subdetectors are investigated: the forward muon detector FMD and the forward tagging system FTS.

The FMD consists of two sets of planar drift chambers in front and behind a toroidal magnet, covering the polar angle region of $3^\circ < \theta < 18^\circ$. The pre–toroid chambers are very effective in detecting secondary particles from interactions of proton remnant particles with the beampipe, collimators, and other material in the forward direction. The relevant observable is the total number of hit pairs in the pre–toroid chambers.

The FTS is a system of 4 sets of scintillator paddles surrounding the proton beam pipe at distances of $26\,\mathrm{m}$, $28\,\mathrm{m}$, $53\,\mathrm{m}$, and $92\,\mathrm{m}$ downstream of the interaction point. Monte Carlo studies indicate that the stations at $26\,\mathrm{m}$ and $28\,\mathrm{m}$ are useful to detect particles from proton dissociation.

Events are considered to be tagged if more than one hit pair in the FMD is observed (a single hit pair being compatible with noise), or if at least one scintillator of the $26\,\mathrm{m}$ or $28\,\mathrm{m}$ FTS stations has detected a particle.

In each W/t bin, the number N_{el} of elastic ρ^0 production events is inferred from the corrected number of ρ^0 events N_cor in this bin, and the fraction of tagged events

$$f_\mathrm{tag} = \frac{N_\mathrm{tag}}{N_\mathrm{tag} + N_\mathrm{untag}}$$

in this W/t bin, where N_tag (N_untag) is the raw number of selected tagged (untagged) events in the mass range $0.6 < m_{\pi\pi} < 1.1$ in the respective W/t bin, using the following relation:

$$N_\mathrm{el} = N_\mathrm{cor} \frac{\epsilon_\mathrm{pd} - f_\mathrm{tag}}{\epsilon_\mathrm{pd} - \epsilon_\mathrm{el}}.$$

Here, ϵ_el (ϵ_pd) is the fraction of selected elastic (proton–dissociative) events that produce a tag, as determined from Monte Carlo simulations. The fractions ϵ_el and ϵ_pd vary with t and are evaluated for the different t bins separately, while they are independent of W and are averaged over the dipion mass range.

4.4 Differential Cross Sections

From the corrected number N_{cor} of ρ^0 events per W/t bin, the differential γp cross section is derived as

$$\frac{\mathrm{d}\sigma^{\gamma\mathrm{p}}(W)}{\mathrm{d}t} = \frac{N_{\mathrm{cor}}}{\int \mathcal{L}\mathrm{d}t\,\Delta t\,\Delta W\,\Phi_{\gamma\mathrm{p}}},$$

where Δt and ΔW are the width in t and W of the respective bin, $\int \mathcal{L}\mathrm{d}t$ is the integrated luminosity, and $\Phi_{\gamma\mathrm{p}}$ is the photon flux factor, integrated up to $Q^2 = 4\,\mathrm{GeV}^2$.

The separate cross sections for elastic and proton-dissociative ρ^0 production are calculated in the same manner, using the number of elastic (proton-dissociative) events N_{el} (N_{pd}).

The W bin centre is evaluated from the arithmetic mean of the W of the events detected in the respective bin. The bin centre in t is calculated according to

$$t_{\text{mean}} = t_{\text{low}} + \frac{1}{b}\cdot(\log(b\cdot\triangle t) - \log(1-\exp(-b\cdot\triangle t)))$$

with $b = 10\,\mathrm{GeV}^{-2}$; at this t_{mean}, the bin averaged cross section is identical to the differential cross section for the chosen b value.

4.5 *W* Dependency and Pomeron Trajectory

The differential γp cross sections measured in the same t range are fitted to the form

$$\frac{\mathrm{d}\sigma^{\gamma\mathrm{p}}(W)}{\mathrm{d}t} = \frac{\mathrm{d}\sigma^{\gamma\mathrm{p}}(W_0)}{\mathrm{d}t}\left(\frac{W}{W_0}\right)^{4(\alpha-1)}, \tag{3}$$

with $W_0 = 37\,\mathrm{GeV}$. The parameter α is, for elastic ρ^0 production, the value of the pomeron trajectory $\alpha = \alpha_{\mathbb{P}}(t)$.

4.6 Systematic Uncertainties

The following sources of systematic uncertainties were considered:

- The W and t dependence of the ρ^0 production cross section.
- The M_{Y} dependence of the proton-dissociative ρ^0 production cross section
- The θ and p_{t} dependence of the FTT single track trigger efficiency
- The tagging efficiencies of the FMD and FTS systems.

For each of these systematic uncertainties, the complete analysis was repeated, and the effect of the corresponding variation on the individual cross sections per bin, the resulting W exponent for fixed t, and the pomeron trajectory was evaluated. Thus, all correlations were fully taken into account.

For the W and t dependence of the ρ^0 production cross section, the intercept of the pomeron trajectory was varied by ± 0.04, its slope vas varied by $\pm 0.25\,\mathrm{GeV}^{-2}$ (corresponding to the extremes of either twice the slope given by Landhoff and Jaroszkiewicz [12] and no shrinkage at all). The b slope parameter was varied by $\pm 10\,\%$ of its value, i.e. by approximately $\pm 1\,\mathrm{GeV}^{-2}$ for elastic and $\pm 0.6\,\mathrm{GeV}^{-2}$ for proton-dissociative events.

For the FTT trigger efficiency, the p_t and θ dependence was varied such that possible systematic trends were covered.

For the forward detectors, the efficiency of the FTS and FMD subdetectors was varied within their uncertainties, and proton-dissociative events were reweighted according to $M_\mathrm{Y}^{\pm 0.3}$ to account for the unknown mass spectrum of the dissociating proton system.

In addition, the following uncertainties that affect the overall normalisation were considered:

- The uncertainty of the luminosity measurement: $1.5\,\%$;
- an uncertainty of $2\,\%$ for the cut on the value of z vertex position;
- the uncertainty of the track reconstruction efficiency: $1.5\,\%$ per track, $3\,\%$ overall;
- the overall uncertainty of the track triggering efficiency: $1.5\,\%$ per track, $3\,\%$ overall;
- the uncertainty of the background contribution: $2\,\%$;
- an additional uncertainty from radiative corrections, for which no corrections were applied: $2\,\%$.

Added in quadrature, this results in an overall normalisation uncertainty of $5.7\,\%$.

5 Results

Fig. 9 shows the differential photoproduction cross sections $\mathrm{d}\sigma/\mathrm{d}t$ for diffractive ρ^0 photoproduction $\gamma p \to \rho^0 Y$ in the kinematic range $(M_\mathrm{Y}^2 + Q^2)/(W^2 + Q^2) < 0.01$ in the different t bins where it was measured.

Fig. 7 shows the same cross section for the elastic process $\gamma p \to \rho^0 p$, in comparison with measurements from the ZEUS collaboration [6, 7]; Fig. 6 shows the same data, which are additionally compared to data from the Omega spectrometer [2] and H1 [4] collaborations. For these comparisons, the data points from the ZEUS and H1 collaborations were corrected to the closest t bin of the present analysis using the t dependence as measured by the respective experiment. For the Omega data, the parametrisation of the measured data as given in [2, Tab. 3] that is valid over the range $0.06 < |t| < 1\,\mathrm{GeV}^2$ was used. For this data, the cross sections were also adjusted (by applying a factor 0.952) to account for the different definition of the ρ^0 cross section that is employed by the Omega collaboration, namely the convention of Spital and Yennie [24]. The data of the present analysis are in good agreement with these previous measurements.

Fig. 8 shows the cross section for the proton-dissociative process $\gamma p \to \rho^0 Y$, again in the range $(M_Y^2 + Q^2)/(W^2 + Q^2) < 0.01$.

Fig. 10 summarizes the measured values of $\alpha\,(t)$ from a fit of the form given in Eq. 3. A straight line fit fit to the observed α values yields for the Pomeron trajectory

$$\alpha_{\mathbb{P}}\,(t) = 1.093 \pm 0.003(stat.)^{+0.008}_{-0.007}(syst.) + (0.116 \pm 0.027(stat.)^{+0.036}_{-0.046}(syst.))\,\mathrm{GeV}^{-2} \cdot t.$$

This result is in excellent agreement with the measurement from the ZEUS collaboration [7], i.e.

$$\alpha_{\mathbb{P}}\,(t) = 1.096 \pm 0.021 + (0.125 \pm 0.038)\,\mathrm{GeV}^{-2} \cdot t,$$

and supports the finding from the ZEUS collaboration that in the space–like region $t < 0$ the Pomeron trajectory, as observed in elastic ρ^0 photoproduction, has a significantly smaller slope than the value of $\alpha'_{\mathbb{P}} = 0.25\,\mathrm{GeV}^{-2}$ derived [12] from other hadron scattering data.

Figs. 11 and 12 show the effective α values of the W dependency for the proton-dissociative and the inclusive diffractive process, respectively.

References

[1] H. R. Crouch *et al.* [Cambridge Bubble Chamber Group], Phys. Rev. **146** (1966) 994;
R. Erbe *et al.* [German Bubble Chamber Collaboration], Nuov. Cim. **46A** (1966) 795;
H. Blechschmidt *et al.*, Nuov. Cim. **52A** (1967) 1348;
J. Ballam *et al.*, Phys. Rev. D **5** (1972) 54; *ibid.* **7** (1973) 3150;
W. Struczinski *et al.* [Aachen-Hamburg-Heidelberg-Munich Collaboration], Nucl. Phys. B **108** (1976) 45;
P. Joos *et al.*, Nucl. Phys. B **113** (1976) 53;
R. W. Clifft *et al.*, Phys. Lett. B **64** (1976) 213;
R. L. Anderson *et al.*, Phys. Rev. D **14** (1976) 679;
S. Bartalucci *et al.*, Nuovo Cim. A **44** (1978) 587;
R. M. Egloff *et al.*, Phys. Rev. Lett. **43**, 657 (1979);
Y. A. Aleksandrov *et al.*, Yad. Fiz. **32** (1980) 651, Sov. J. Nucl. Phys. **32** (1980) 334;
M. Atkinson *et al.* [Omega Photon Collaboration], Nucl. Phys. B **245** (1984) 189;
R. J. Apsimon *et al.* [Omega Photon Collaboration], Z. Phys. C **53** (1992) 581;
M. R. Adams *et al.* [E665 Collaboration], Z. Phys. C **74** (1997) 237;
C. Wu *et al.*, Eur. Phys. J. A **23** (2005) 317.

[2] D. Aston *et al.*, Nucl. Phys. B **209** (1982) 56.

[3] M. Derrick *et al.* [ZEUS Collaboration], Z. Phys. C **69** (1995) 39.

[4] S. Aid *et al.* [H1 Collaboration], Nucl. Phys. B **463** (1996) 3.

[5] M. Derrick *et al.* [ZEUS Collaboration], Z. Phys. C **73** (1997) 253.

[6] J. Breitweg *et al.* [ZEUS Collaboration], Eur. Phys. J. C **2** (1998) 247.

[7] J. Breitweg *et al.* [ZEUS Collaboration], Eur. Phys. J. C **14** (2000) 213.

[8] J. J. Sakurai, Annals Phys. **11** (1960) 1; *idem*, Phys. Rev. Lett. **22** (1969) 981;
M. Gell-Mann and F. Zachariasen, Phys. Rev. **124** (1961) 953;
T. H. Bauer, R. D. Spital, D. R. Yennie and F. M. Pipkin, Rev. Mod. Phys. **50** (1978) 261 [Erratum-ibid. **51** (1979) 407].

[9] T. Regge, Nuovo Cim. **14** (1959) 951; *ibid.* **18** (1960) 947.

[10] A. Donnachie and P. V. Landshoff, Phys. Lett. B **296** (1992) 227.

[11] J. R. Cudell, K. Kang and S. K. Kim, Phys. Lett. B **395** (1997) 311.

[12] G. A. Jaroszkiewicz and P. V. Landshoff, Phys. Rev. D **10**, 170 (1974);
P. V. Landshoff, Nucl. Phys. Proc. Suppl. **12** (1990) 397.

[13] I. Abt *et al.* [H1 Collaboration], Nucl. Instrum. Meth. A **386** (1997) 310; *ibid.* 348;
R. D. Appuhn *et al.* [H1 SPACAL Group], Nucl. Instrum. Meth. A **386** (1997) 397.

[14] R. Weber, "Diffractive ρ^0-photoproduction at H1," PhD thesis ETH Zurich 2006, in preparation.

[15] A. Baird *et al.*, IEEE Trans. Nucl. Sci. **48** (2001) 1276 [arXiv:hep-ex/0104010];
A. Baird *et al.* [H1 Collaboration], Nucl. Instrum. Meth. A **461** (2001) 461;
A. Schöning [H1 Collaboration], Nucl. Instrum. Meth. A **518** (2004) 542;
N. Berger *et al.*, Nucl. Sc. Symp. Conf. Rec., 2004 IEEE, **3** (2004) 1976.

[16] B. List and A. Mastroberardino, "DIFFVM: A Monte Carlo generator for diffractive processes in e p scattering," *Prepared for Workshop on Monte Carlo Generators for HERA Physics (Plenary Starting Meeting), Hamburg, Germany, 27-30 Apr 1998* DESY-PROC-1999-02 (1999) 396.

[17] C. F. von Weizsäcker, Z. Phys. **88** (1934) 612;
E. J. Williams, Phys. Rev. **45** (1934) 729;
V. M. Budnev, I. F. Ginzburg, G. V. Meledin and V. G. Serbo, Phys. Rept. **15** (1974) 181.

[18] K. Goulianos, Phys. Rept. **101** (1983) 169.

[19] S. Eidelman *et al.* [Particle Data Group], Phys. Lett. B **592** (2004) 1.

[20] T. Sjöstrand, Comput. Phys. Commun. **39** (1986) 347; *idem*, arXiv:hep-ph/9508391;
T. Sjöstrand and M. Bengtsson, Comput. Phys. Commun. **43** (1987) 367.

[21] M. Ross and L. Stodolsky, Phys. Rev. **149** (1966) 1172.

[22] P. Söding, Phys. Lett. **19** (1966) 702.

[23] J. D. Jackson, Nuovo Cim. **34** (1964) 1644.

[24] R. Spital and D. R. Yennie, Phys. Rev. D **9**, 126 (1974).

[25] A. Abele *et al.* [CRYSTAL BARREL Collaboration], Eur. Phys. J. C **21** (2001) 261.

[26] A. B. Clegg and A. Donnachie, Z. Phys. C **62** (1994) 455.

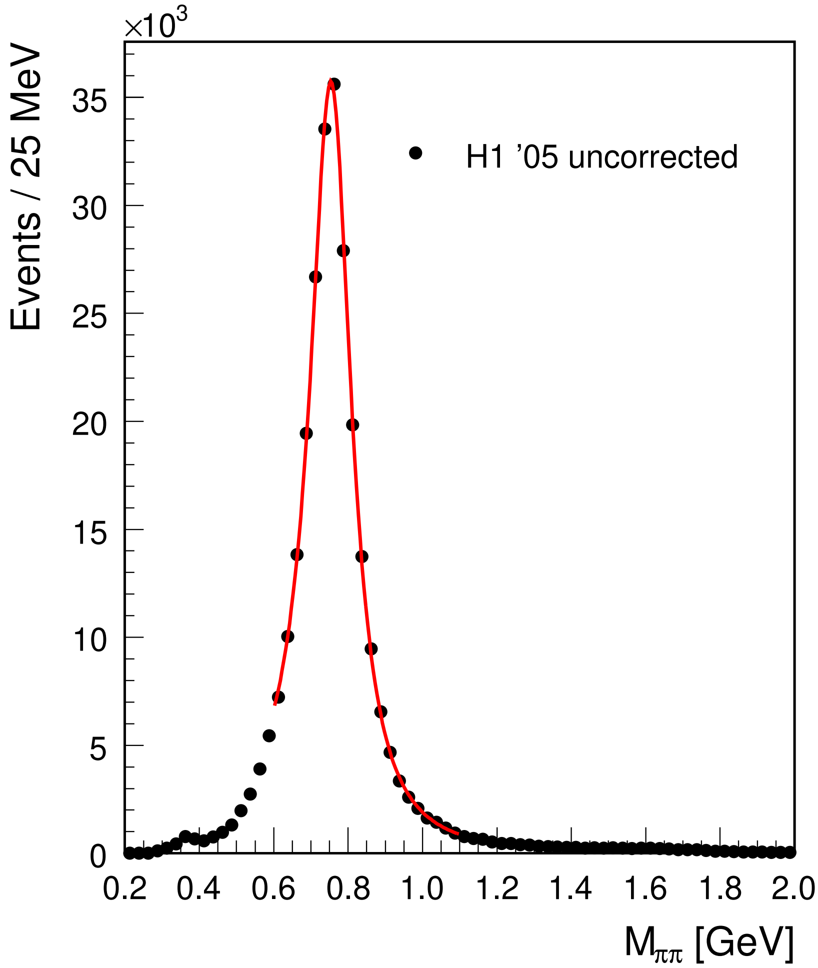

Figure 1: The dipion mass spectrum of the selected candidate events. The spectrum is fitted with a skewed relativistic Breit-Wigner function according to Eq. (2) to guide the eye.

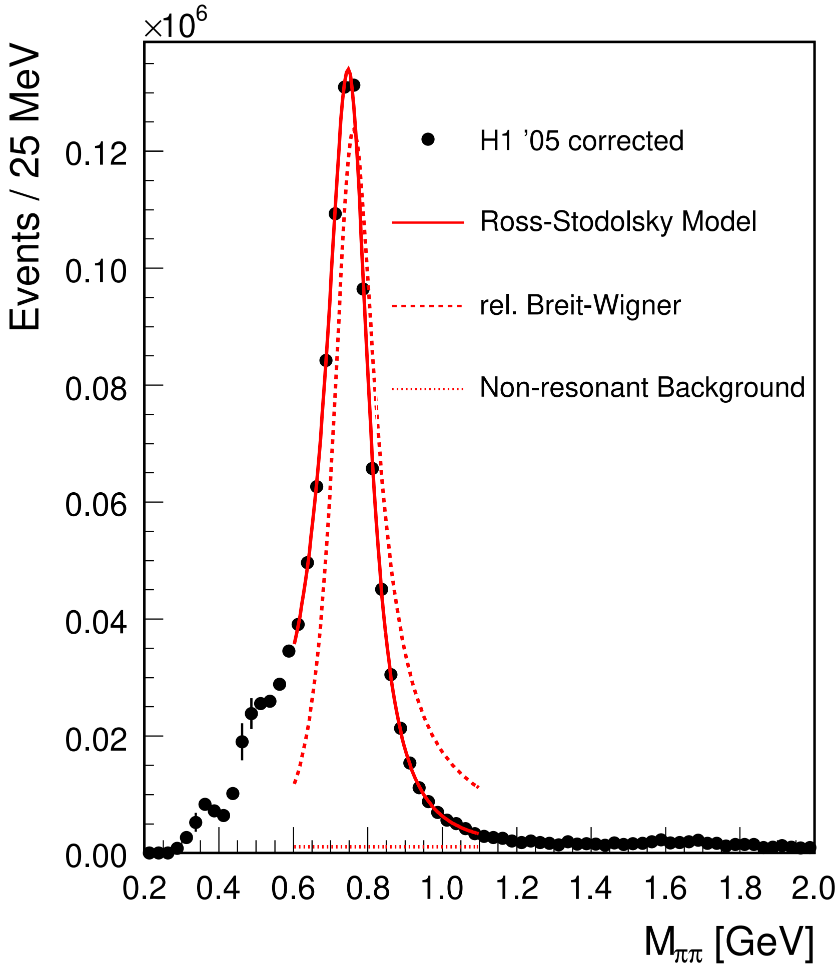

Figure 2: The dipion mass spectrum of the selected candidate events, corrected for acceptance, reconstruction and trigger efficiencies, with a fit according to Eq. 2. The dashed lines show the contributions from the background and the unskewed relativistic Breit–Wigner distribution.

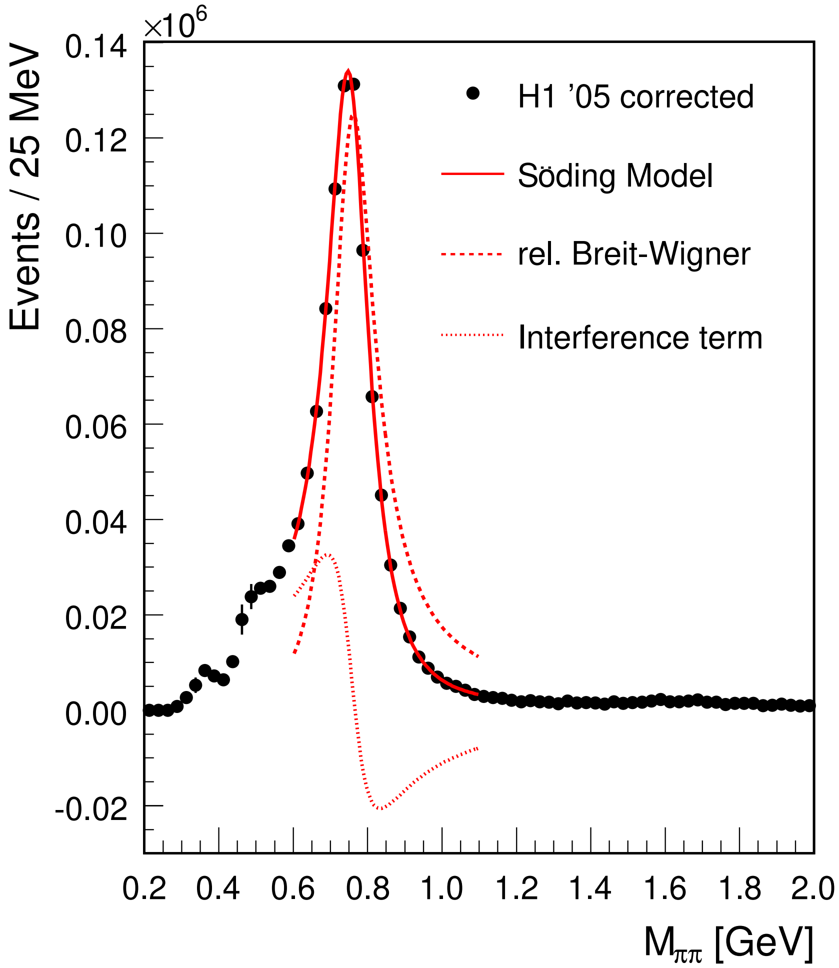

Figure 3: The dipion mass spectrum of the selected candidate events, corrected for acceptance, reconstruction and trigger efficiencies, with a fit according to Eq. 1. The dashed lines show the contributions from the interference term and the unskewed relativistic Breit–Wigner distribution. The background term is set to 0.

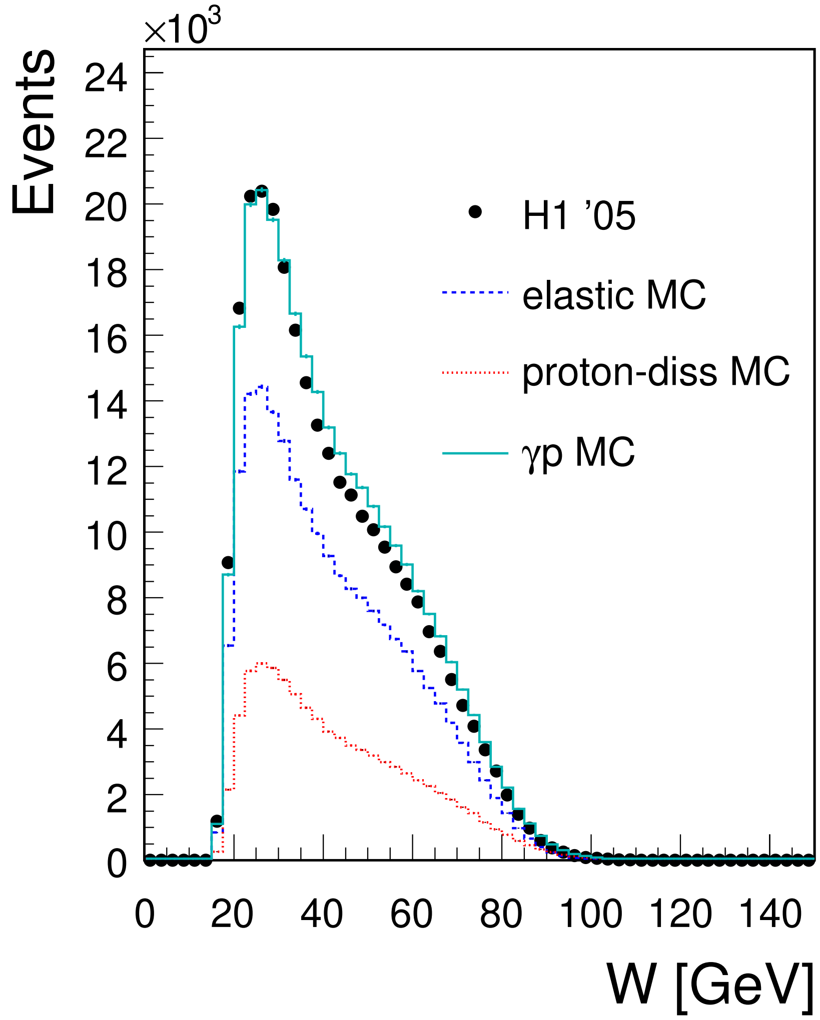

Figure 4: The W spectrum of the selected events, compared to the Monte Carlo prediction.

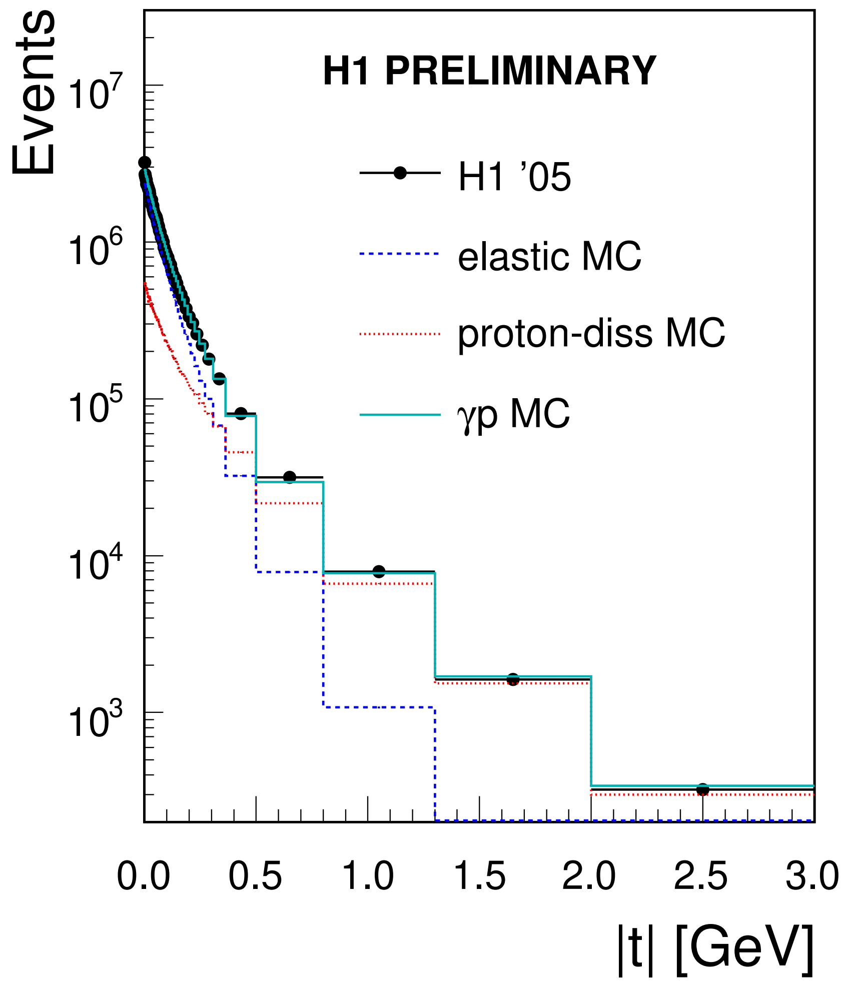

Figure 5: The t spectrum of the selected events, compared to the Monte Carlo prediction.

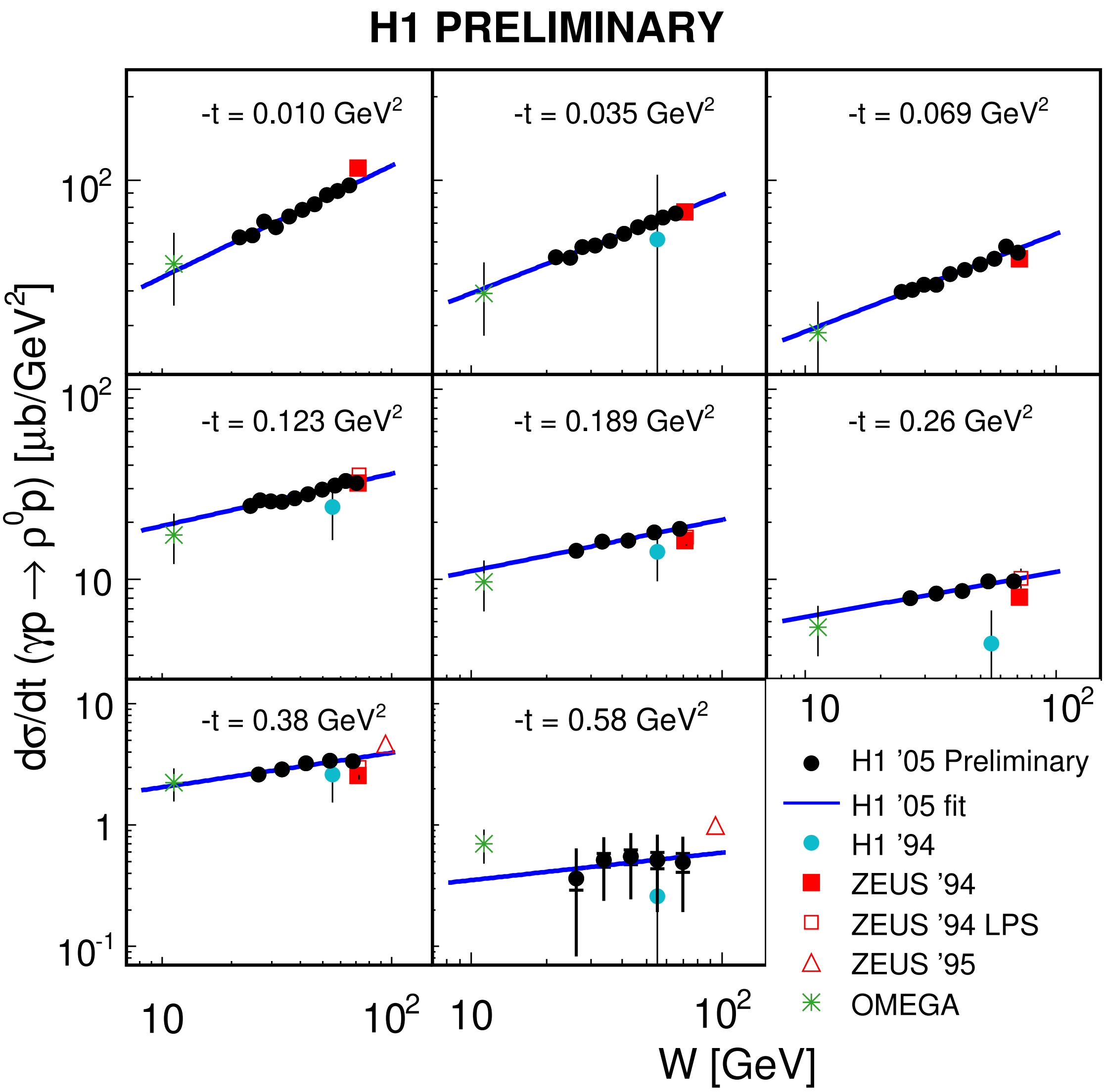

Figure 6: The measured γp cross sections for elastic ρ^0 photoproduction $\gamma p \to \rho^0 p$, for different values of t. The measurent is compared to results from other experiments [2, 4, 5, 6, 7]. The lines show the result of a fit $\mathrm{d}\sigma/\mathrm{d}t = a(W/W_0)^{4[\alpha(t)-1]}$ to the data of the current analysis, with $W_0 = 37\,\mathrm{GeV}$; the fit result is extrapolated for better comparison with the data from other experiments.

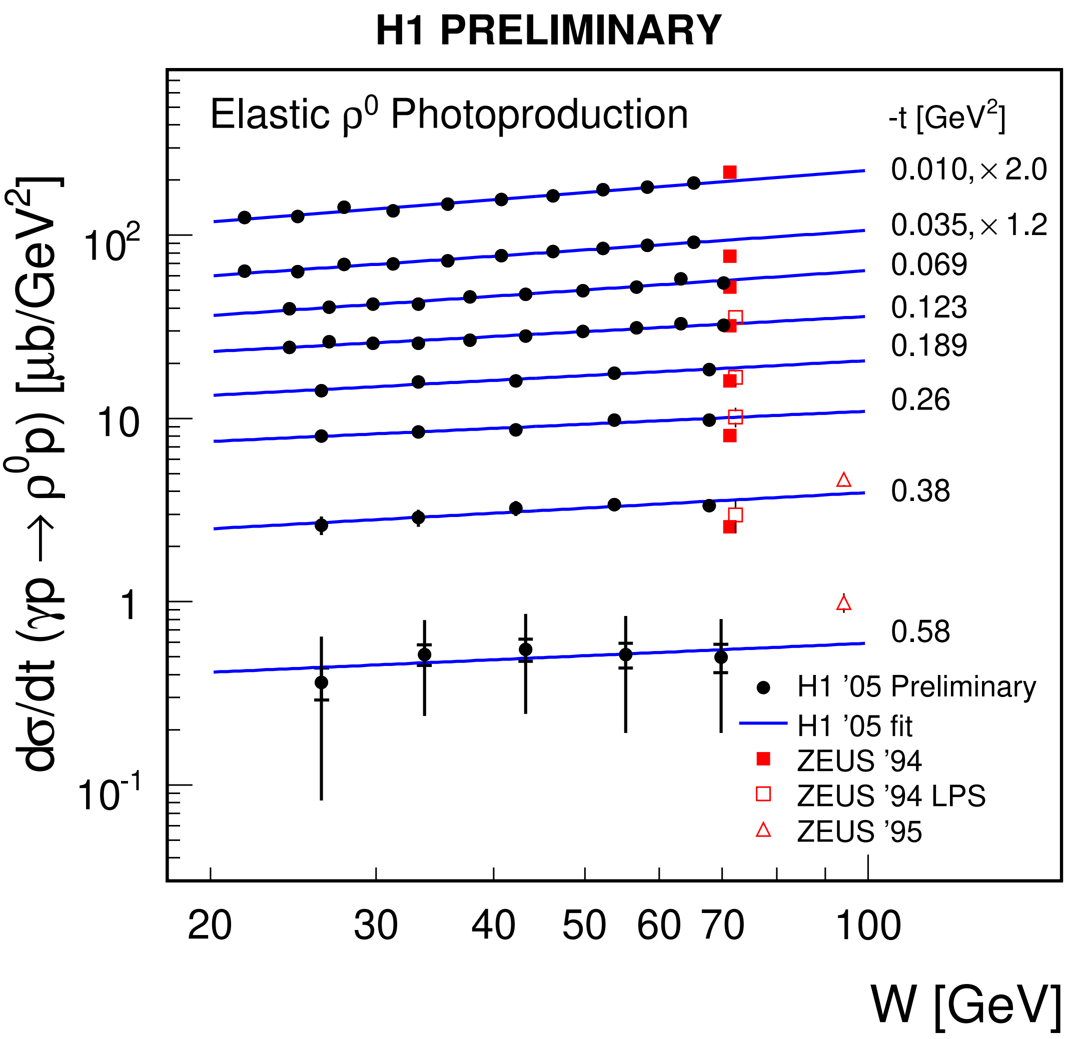

Figure 7: The measured γp cross sections for elastic ρ^0 photoproduction $\gamma p \rightarrow \rho^0 p$, for different values of t. The measurent is compared to results from other experiments [5, 6, 7].

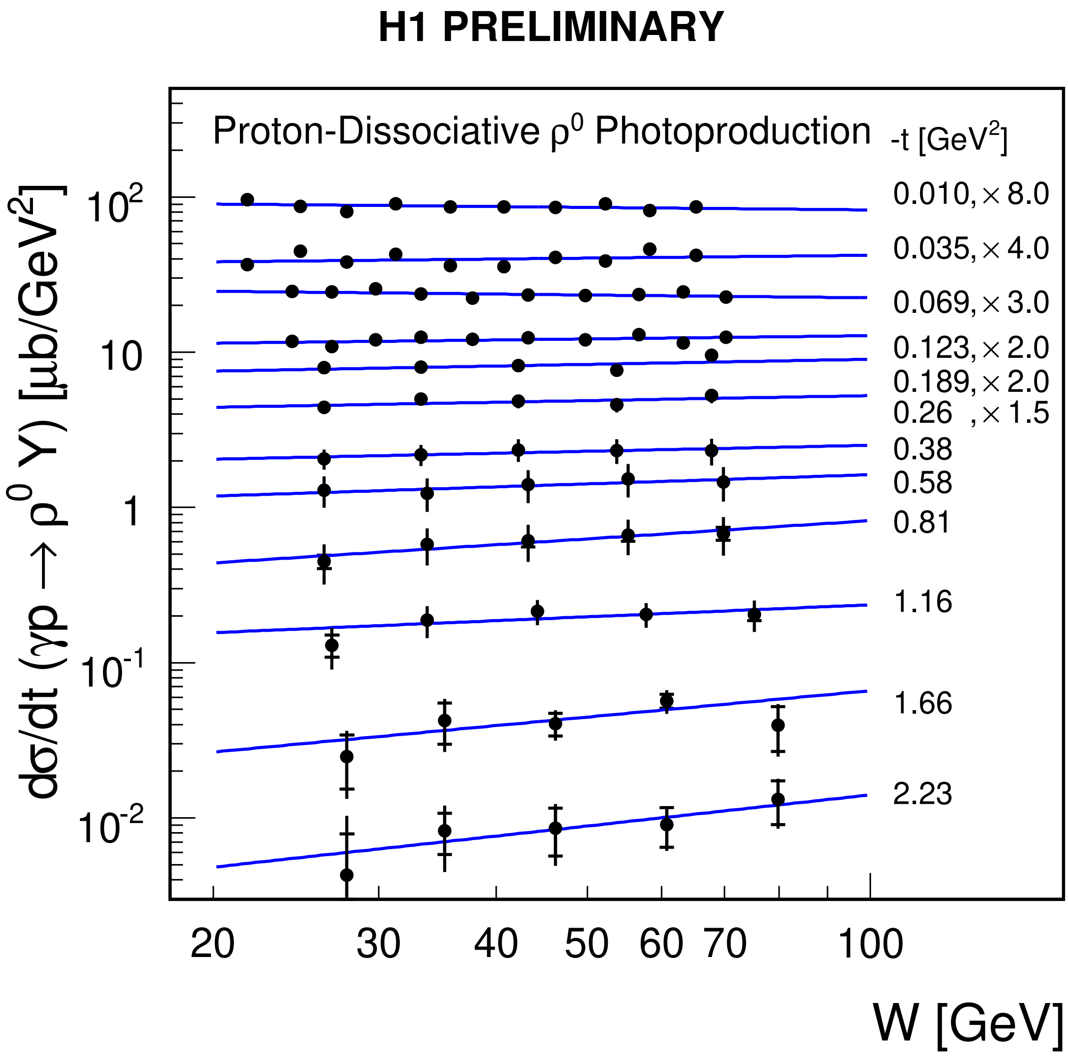

Figure 8: The measured γp cross sections for proton-dissociative ρ^0 photoproduction $\gamma p \to \rho^0 Y$, in the range $(M_Y^2 + Q^2)/(W^2 + Q^2) < 0.01$, for different values of t.

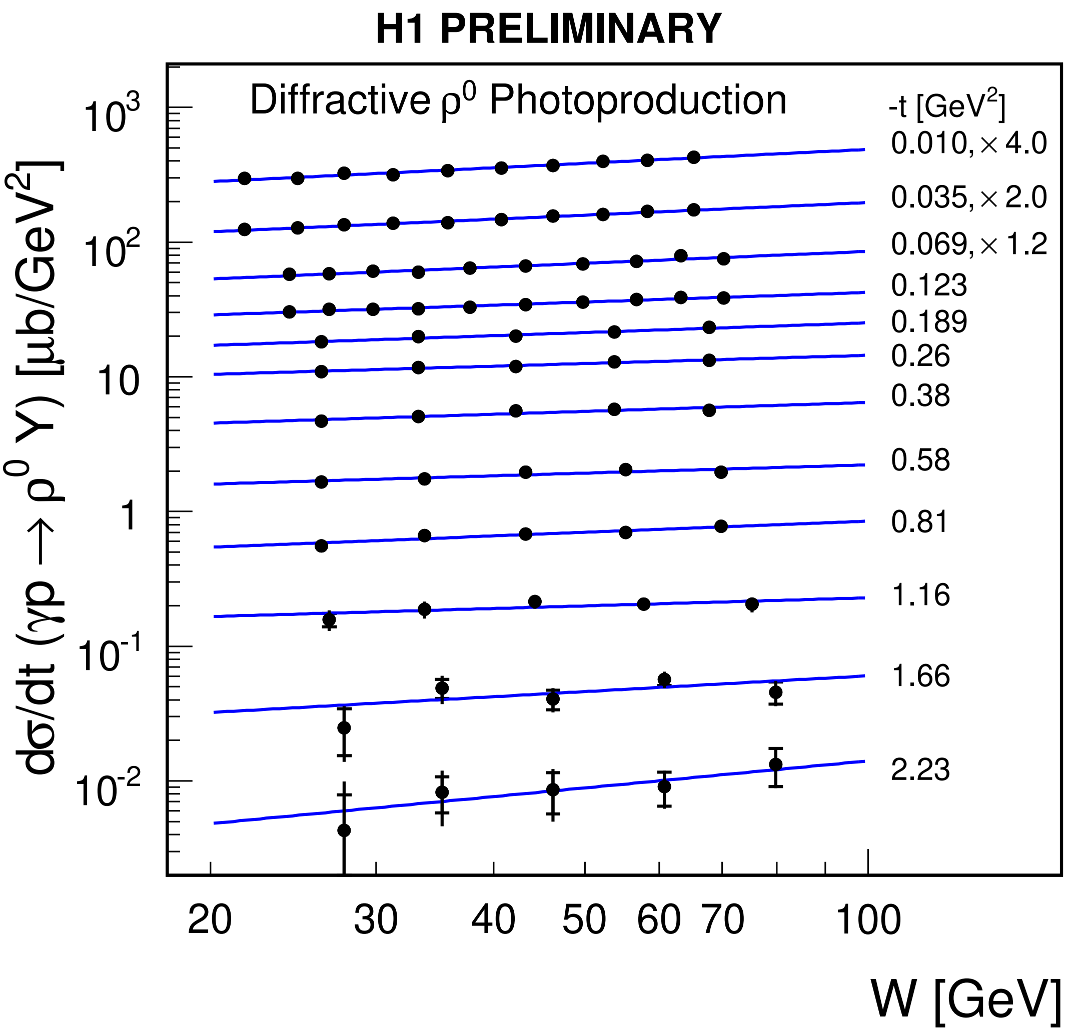

Figure 9: The measured γp cross sections for diffractive ρ^0 photoproduction $\gamma p \to \rho^0 Y$, in the range $(M_\mathrm{Y}^2 + Q^2)/(W^2 + Q^2) < 0.01$, for different values of t.

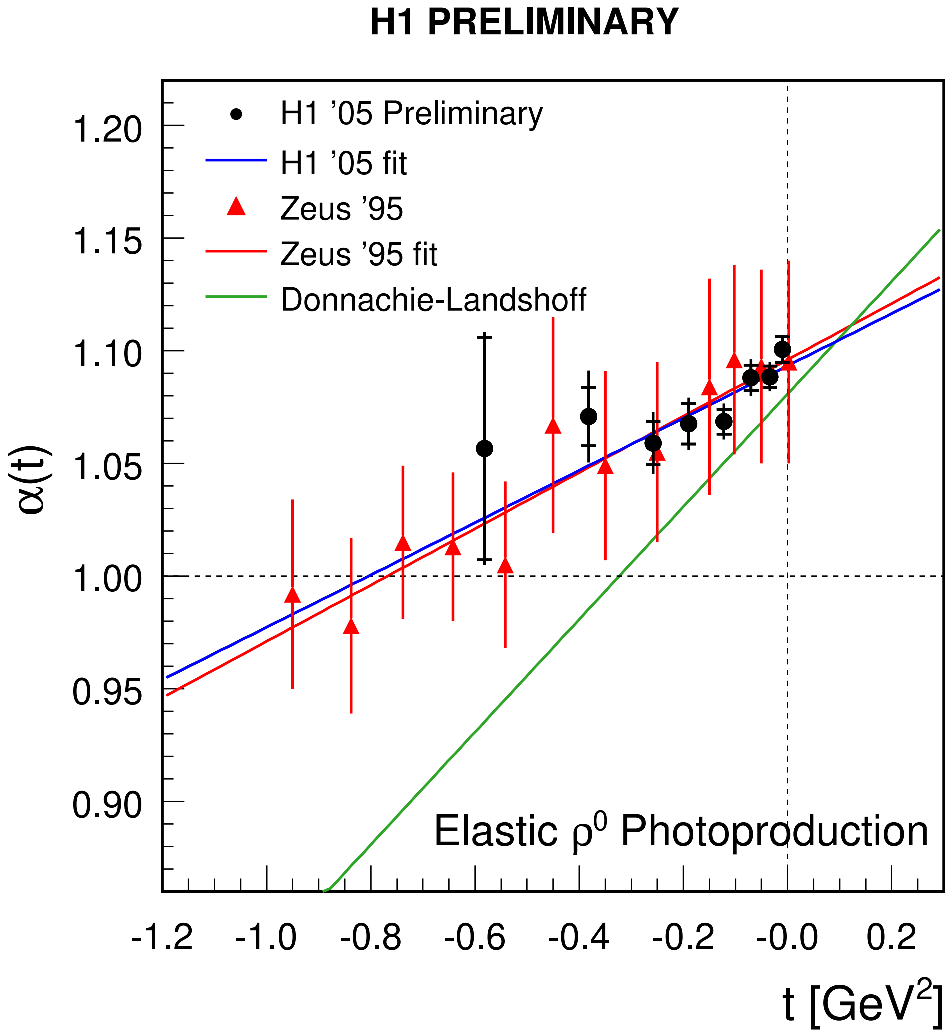

Figure 10: The measured values of the α parameter for elastic ρ^0 photoproduction, together with a fit to the Pomeron trajectory of the form $\alpha_{\mathbb{P}}(t) = \alpha_{\mathbb{P},0} + \alpha'_{\mathbb{P}} \cdot t$, with $\alpha_{\mathbb{P},0} = 1.093 \pm 0.003(stat.)^{+0.008}_{-0.007}(syst.)$ and $\alpha'_{\mathbb{P}} = (0.116 \pm 0.027(stat.)^{+0.036}_{-0.046}(syst.))$ GeV^{-2}. The result from the ZEUS collaboration [7] is also shown, as well as the parametrisation from Donnachie and Landshoff [10, 12]

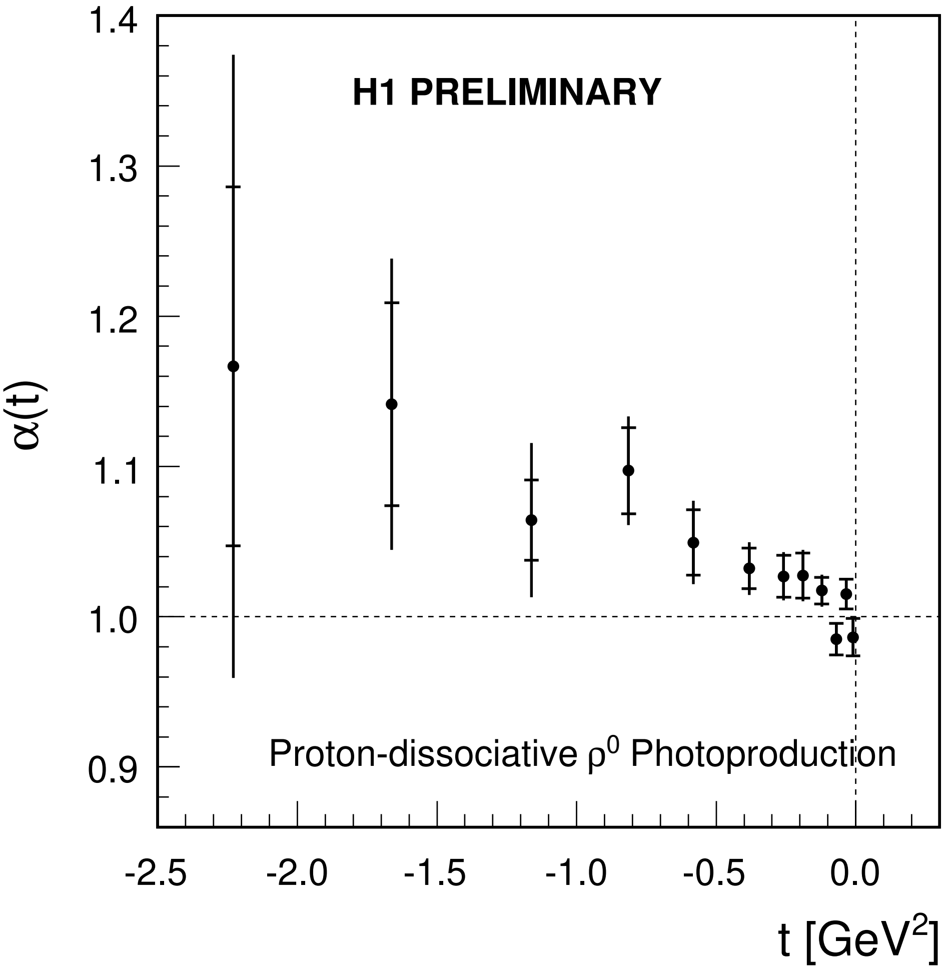

Figure 11: The measured values of the α parameter of the W dependency for proton-dissociative ρ^0 photoproduction.

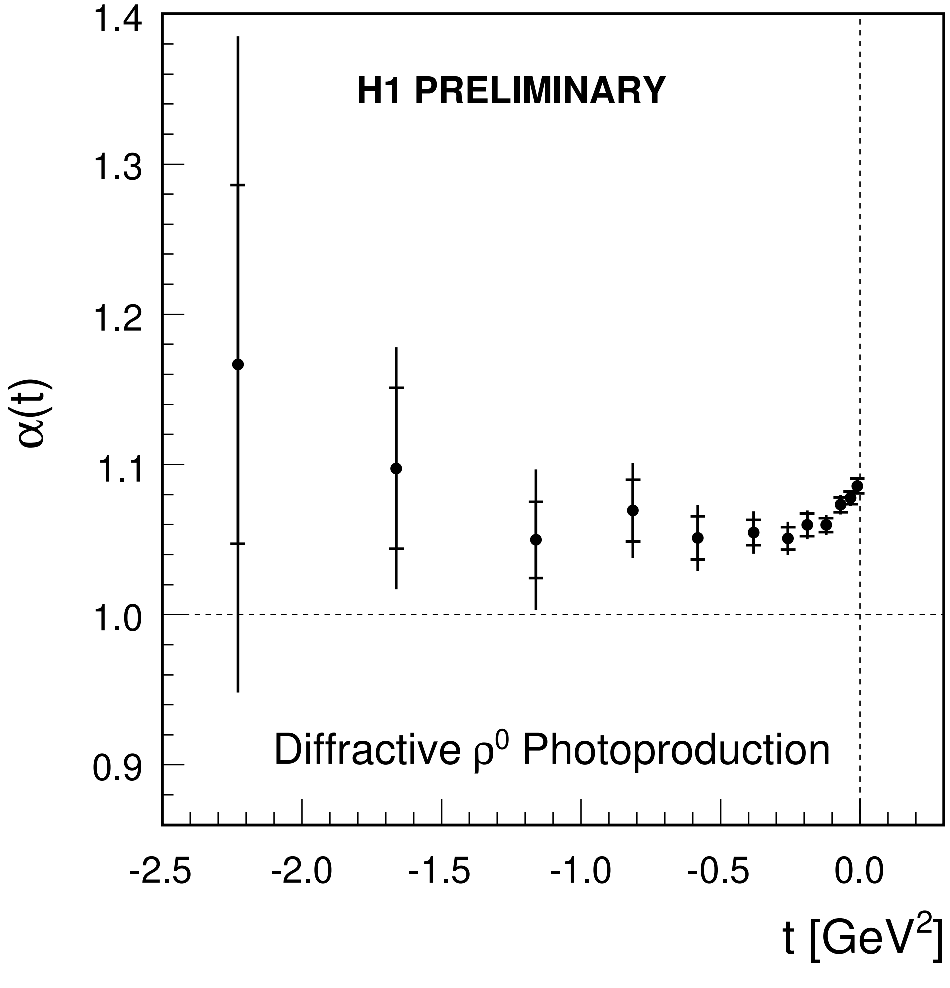

Figure 12: The measured values of the α parameter of the W dependency for diffractive, i.e. elastic and proton-dissociative, ρ^0 photoproduction.